

Supporting Information for: Controlled Pore Generation in Single Layer Graphene Oxide for Membrane Desalination

Federico Raffone,* Filippo Savazzi, and Giancarlo Cicero

*Dipartimento di Scienza Applicata e Tecnologia, Politecnico di Torino, Corso Duca degli
Abruzzi 24, Torino 10129, Italy*

E-mail: federico.raffone@polito.it

Pair interaction on graphene sheet

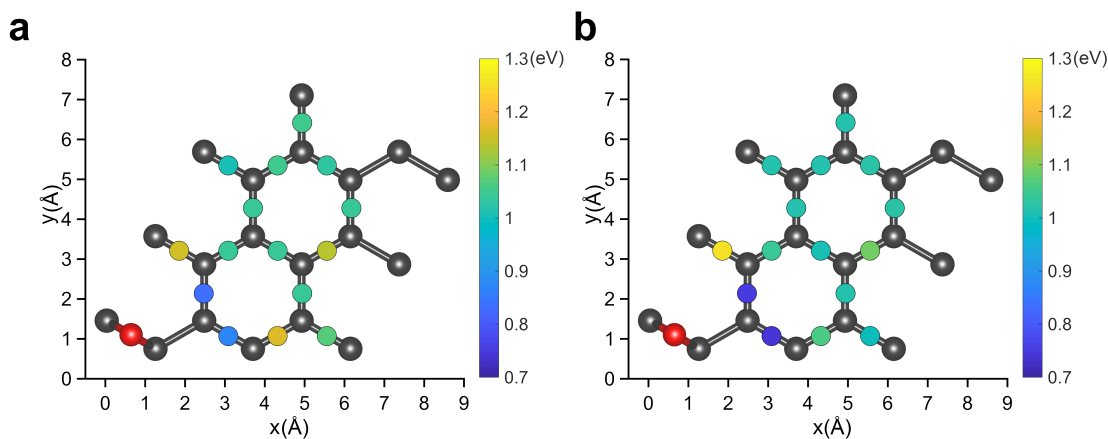


Figure S1: Formation energy of pairs of epoxides on the same side (a) or on different sides (b) of the GO layer. The carbon atoms are shown in gray while the red atom represents the reference epoxide group. The colour of each remaining ball indicates the formation energy in eV of the pair constituted by an epoxide located at the ball position and the reference epoxide. The minimal difference between the two pictures suggests that it is unimportant whether the epoxides lie all on one side of the graphene layer or not. It is then possible to reduce the complexity of the simulations treating only one side of the graphene layer.

Cluster Expansion figures

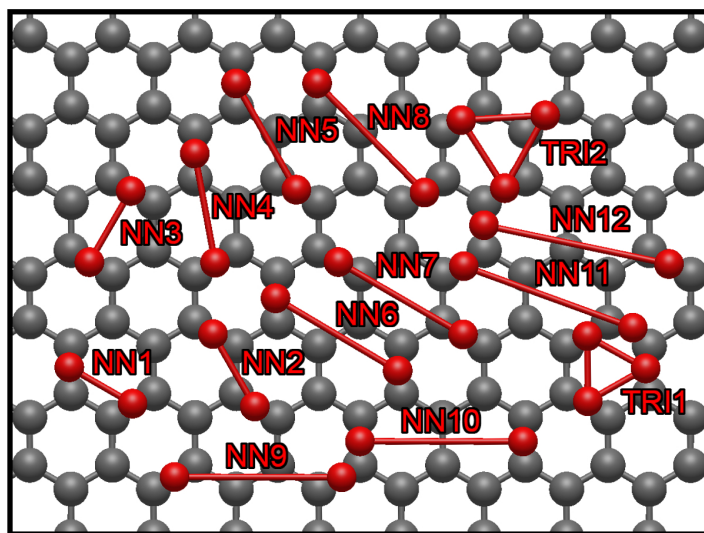


Figure S2: Figures used to fit the energy of a GO sheet.

Table S1: ECIs used in the Cluster Expansion. The nomenclature refers to Supplementary Figure 2.

| ECI figure | Energy (eV) |
|------------|-------------|
| H_0 | -103.356 |
| h_i | -433.382 |
| J_{NN1} | -0.539 |
| J_{NN2} | -0.373 |
| J_{NN3} | -0.116 |
| J_{NN4} | 0.014 |
| J_{NN5} | 0.096 |
| J_{NN6} | -0.024 |
| J_{NN7} | -0.281 |
| J_{NN8} | -0.046 |
| J_{NN9} | 0.023 |
| J_{NN10} | -0.177 |
| J_{NN11} | 0.063 |
| J_{NN12} | -0.134 |
| J_{TRI1} | 0.254 |
| J_{TRI2} | 0.176 |

Coverage dependent barrier

The energy barrier E_{bar} , either forward E_{fwd} or reverse E_{rev} , of a thermally activated process is affected by the epoxide-epoxide interactions as shown in Supplementary Fig. 3.

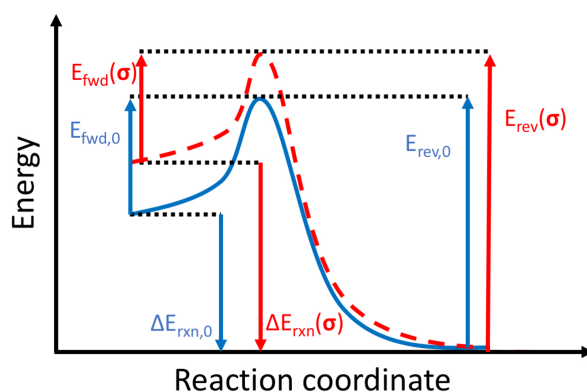


Figure S3: Potential profile of a thermally activated process in the zero-coverage limit (blue) and considering epoxide-epoxide interactions (red).

In the Fig. $\Delta E_{rxn}(\sigma)$ is the difference between the energy of the initial state and the

final state considering lateral interactions. The state energies can be extracted using CE. The height of the forward process barrier can be then obtained as follows:

$$E_{fwd}(\boldsymbol{\sigma}) = \max(0, \Delta E_{rxn}(\boldsymbol{\sigma}), E_{fwd,0} + \omega(\Delta E_{rxn}(\boldsymbol{\sigma}) - \Delta E_{rxn,0})) \quad (1)$$

where $E_{fwd,0}$ is the barrier in the zero-coverage limit, $\Delta E_{rxn,0}$ is the difference between the initial and the final state energy in the zero-coverage limit and ω is the proximity factor indicating the location of the transition state in reaction coordinates (0 for initial-state-like transition state, 1 for final-state-like transition state). In our simulations we have taken $\omega = 0.5$. Analogously, the reverse barrier can be written as:

$$E_{rev}(\boldsymbol{\sigma}) = \max(-\Delta E_{rxn}(\boldsymbol{\sigma}), 0, E_{rev,0} + (1 - \omega)(\Delta E_{rxn}(\boldsymbol{\sigma}) - \Delta E_{rxn,0})) \quad (2)$$

Cluster size density evolution over time

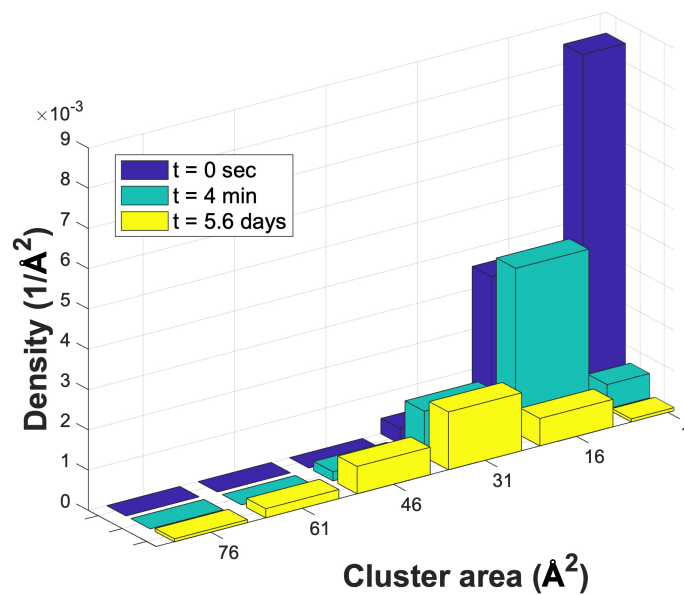


Figure S4: Cluster size density distribution in a GO monolayer with an oxygen coverage of 5% annealed at 300 K for 0 seconds (blue columns), 4 minutes (green columns) and 5.6 days (yellow columns).

Coverage effect

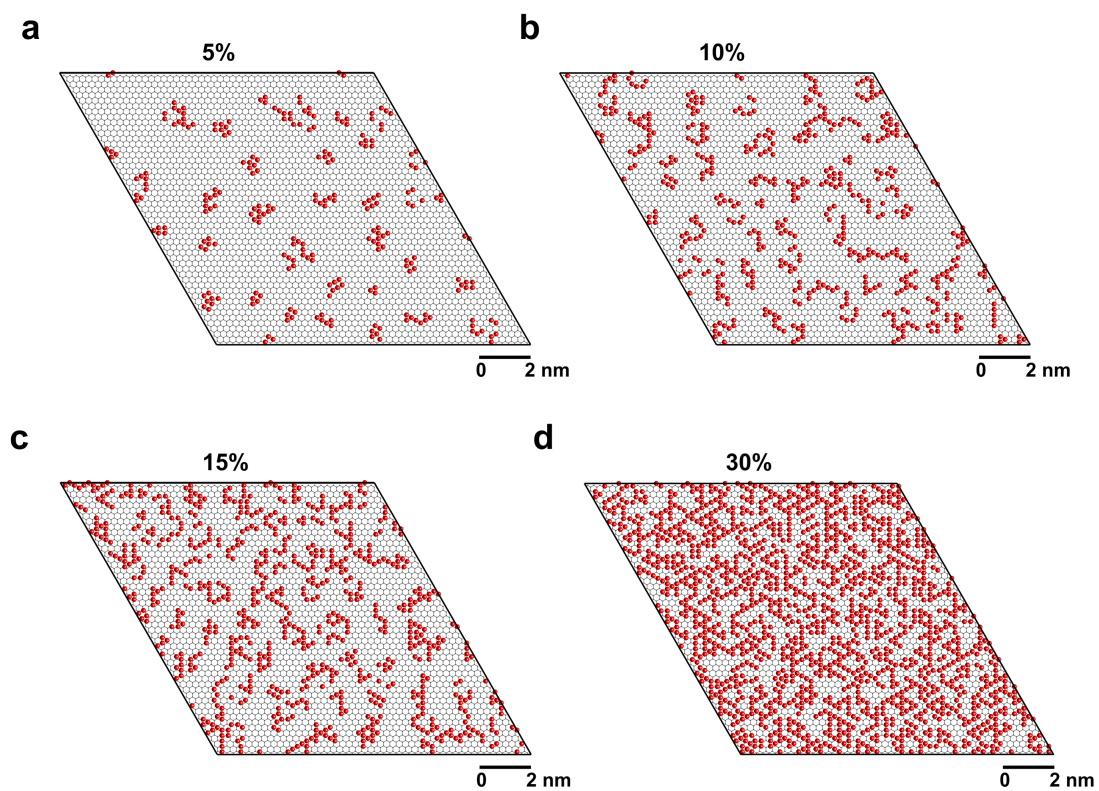


Figure S5: Comparison among GO monolayers with an oxygen coverage of 5% (a), 10% (b), 15% (c) and 30% (d) after 2 days of mild annealing at 300 K.

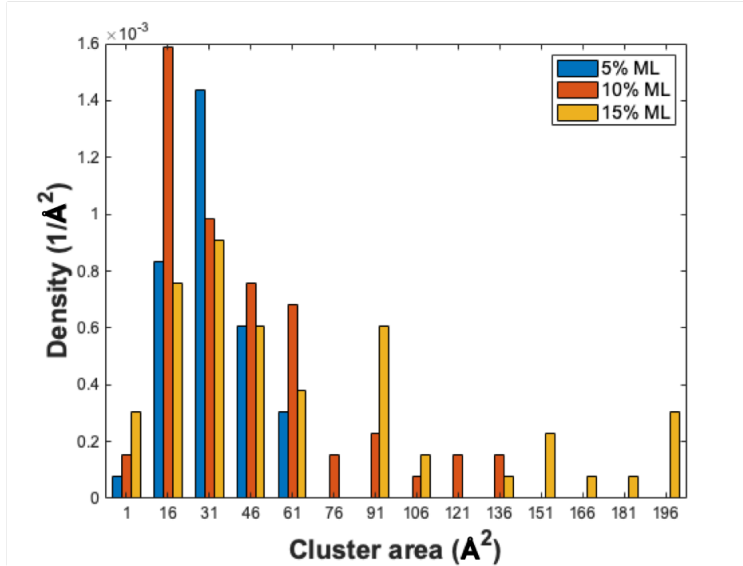


Figure S6: Cluster size distribution of three GO monolayers with an oxygen coverage of 5% (blue), 10% (orange), 15% (yellow) after 2 days of mild annealing at 300 K.

In Fig. S5 we show the comparison of the results of four simulations at different initial GO oxygen coverages (5%, 10%, 15% and 30%) after two days of simulated annealing at 300 K. As the coverage increases the clusters become larger with a more linear shape. The calculated roundness of the clusters at 5%, 10%, 15% coverage is 1.5, 1.8, 2.6 respectively. As described in the main text, epoxides were considered part of a cluster if their interdistance was below 4 Å. At 30% coverage clusters are interconnected throughout the whole sheet and, thus, no statistics is provided. In Fig. S6, the density distribution of the cluster size present in Fig. S5 is plotted. The distribution of the 5% coverage has a particularly sharp gaussian-like distribution. There is no sign of a single dominating cluster which would create an oversize pore compromising the selectivity of the graphene membrane. At higher coverages, especially at 15%, the distribution becomes broader.

Diffusion barrier variation

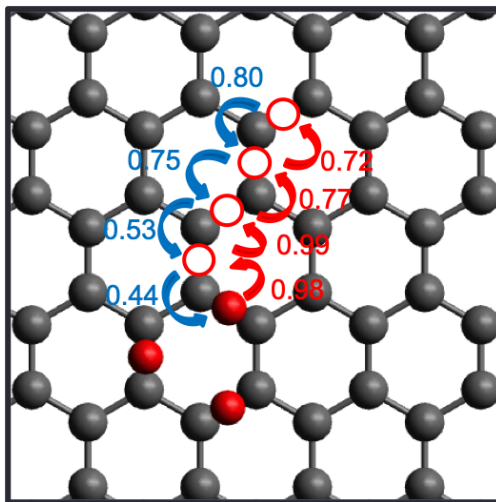


Figure S7: Diffusion barrier of an oxygen approaching a pair of epoxides. Numbers represent the barrier height in eV.

The effect of the proximity of an epoxide pair on a third single epoxide is shown in Fig. S7. When the single epoxide is far from the pair the barriers to move toward or away from the pair are similar. However, when the oxygen is closer the diffusion toward the pair becomes easier thus the cluster formation gets highly favorable. The formed clusters are rather stable even if formed by only three epoxides. That is indicating that the formation of a larger cluster is a slow process as for it to occur the highly endothermic detachment of single epoxides from small cluster is needed. To more consistently prove this point, we show in Fig. S8 the escape barriers of an epoxide for three different small clusters. For all of them, the escape barrier is above 0.90 eV while the reverse process is decisively favored.

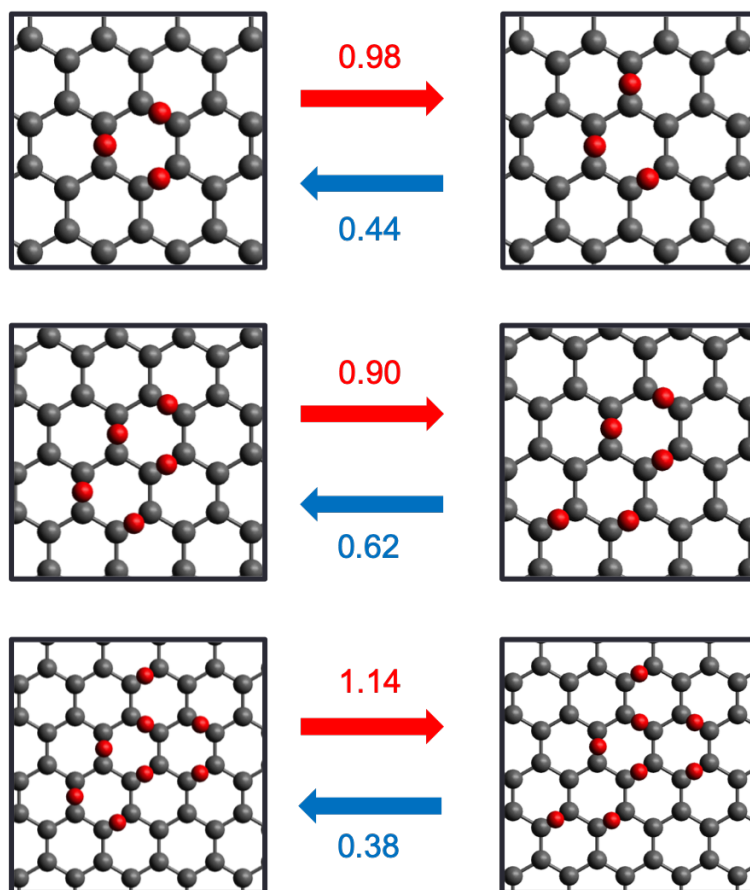


Figure S8: Diffusion barrier of an oxygen approaching a pair of epoxides. Numbers represent the barrier height in eV.

Reducing process effects on an early clustered GO layer

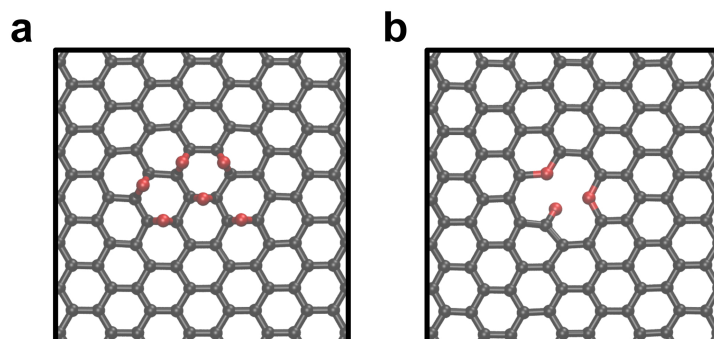


Figure S9: Example of the effect of a high temperature reducing process on a portion of the GO layer that has been annealed for only 4 minutes. Panel (a) shows a small epoxide cluster before the reducing treatment while panel (b) after the treatment.

Molecular dynamics method

To predict the effects of a high temperature reducing process, we performed classical molecular dynamics simulations on a portion of the clustered GO layers obtained from KMC. A single clustered oxidized area surrounded by pristine graphene was included in a $4.3 \text{ nm} \times 4.5 \text{ nm} \times 9.0 \text{ nm}$ supercell. Periodic boundaries conditions were applied in all directions. The structure was heated for 500 ps at a temperature of 2500 K, higher compared to experiments to simulate the process within the timescale of classical molecular dynamics, similarly to Ref.,¹ than thermalized at 300 K for other 40 ps. The temperature was controlled by means of the Nosé-Hover thermostat with a damping factor of 100 timesteps. An energy minimization was performed before and after the dynamics. To catch the bond breaking/formation a Reax force field was employed² with a timestep of 0.1 fs. All MD simulations were performed with the LAMMPS software.³

Density Functional Theory method

Density Functional Theory simulations for the fitting of the Cluster Expansion were carried out in the PBE formulation⁴ of the General Gradient Approximation.⁵ Plane-waves basis set was employed with 36 Ry cutoff for the wave functions and 360 Ry for the densities. The pseudopotentials used in the calculations were ultrasoft.⁶ With these parameters, the resulting C-C bond in graphene was 1.43 Å. The graphene and GO sheets were represented in slabs having 10 Å of vacuum layer separating periodic replicas. For the graphene unit cell, a $(14 \times 14 \times 1)$ Monkhorst-Pack grid was used for the Brillouin zone sampling that was reduced accordingly when the supercell size increased. To obtain the GO structures, a relaxation of both the supercell and the atomic position was performed. The calculations were considered converged when forces on the atoms were smaller than 26 meV/Å and the pressure on the cell was smaller than 0.001 Kbar. All computation were performed with the QUANTUM ESPRESSO software package.⁷

Acknowledgement

We acknowledge the CINECA award under the ISCRA initiative and HPC@POLITO for the availability of high-performance computing resources and support. This work is part of the "DESAL" project funded by Politecnico di Torino. The authors declare no competing financial interests.

References

- (1) Lin, L.-C.; Grossman, J. C. Atomistic understandings of reduced graphene oxide as an ultrathin-film nanoporous membrane for separations. *Nat. Commun.* **2015**, *6*, 8335.
- (2) Chenoweth, K.; van Duin, A. C.; Goddard, W. A. ReaxFF reactive force field for molecular dynamics simulations of hydrocarbon oxidation. *J. Phys. Chem. A* **2008**, *112*, 1040–1053.
- (3) Plimpton, S. Fast parallel algorithms for short-range molecular dynamics. *J. Comput. Phys.* **1995**, *117*, 1–19.
- (4) J. P. Perdew, K. B.; Ernzerhof, M. Generalized gradient approximation made simple. *Phys. Rev. Lett.* **1996**, *77*, 3865.
- (5) Langreth, D. C.; Perdew, J. P. Theory of nonuniform electronic systems. I. Analysis of the gradient approximation and a generalization that works. *Phys. Rev. B* **1980**, *21*, 5469.
- (6) Vanderbilt, D. Soft self-consistent pseudopotentials in a generalized eigenvalue formalism. *Phys. Rev. B* **1990**, *41*, 7892.
- (7) Giannozzi, P.; Baroni, S.; Bonini, N.; Calandra, M.; Car, R.; Cavazzoni, C.; Ceresoli, D.; Chiarotti, G. L.; Cococcioni, M.; Dabo, I. et al. *J. Phys. Condens. Mat.* **2009**, *21*, 395502.